

# **EVALUATION OF SEISMIC DEFORMATION DEMANDS USING NON-LINEAR PROCEDURES IN MULTISTORY STEEL AND CONCRETE MOMENT FRAMES**

Sashi K. Kunnath and Erol Kalkan

Department of Civil and Environmental Engineering  
University of California at Davis  
Davis, CA 95616, U.S.A.

## **ABSTRACT**

A key component of performance-based seismic evaluation is the estimation of seismic demands. In FEMA-356 (FEMA, 2000b), which is now recognized as the model for future performance-based seismic codes in the US, these demands are evaluated at the component level in terms of ductility demands or plastic rotations when using non-linear procedures. Since acceptance criteria for various performance objectives are assessed in terms of local component demands, it is essential that a rational basis be established for determining such demands. Of the non-linear procedures advocated in FEMA-356, pushover procedures are becoming increasingly popular in engineering practice. However, there are still several unresolved issues in identifying appropriate lateral load patterns to be used in a pushover procedure. This paper investigates the correlation between demand estimates for various lateral load patterns used in non-linear static analysis. It also examines the rationale for using component demands over story and system demands. Results reported in the paper are based on a comprehensive set of pushover and non-linear time-history analyses carried out on eight- and twelve-story steel and concrete moment frames. Findings from this study point to inconsistencies in the demands predicted by different lateral load patterns when using pushover analysis and also highlight some issues in the current understanding of local demand estimates using FEMA-based procedures.

**KEYWORDS:** Ductility Demand, Lateral Load Patterns, Non-linear Analysis, Performance-Based Seismic Design, Pushover Analysis

## **INTRODUCTION**

It is now widely recognized that the concepts and guidelines embodied in FEMA-356 contain the essential ingredients of a performance-based seismic design (PBSD) procedure. Though this document was developed for use in seismic rehabilitation of existing buildings, the key elements of the methodology are designed to accommodate the provisions of a future performance-based standard. FEMA-356 is essentially a deterministic approach to PBSD. FEMA-350 (FEMA, 2000a), on the other hand, is a guideline for new steel construction and contains a probabilistic approach to performance assessment. ATC (1996) shares many common elements with FEMA-356 but is limited in scope to reinforced concrete buildings. There are other ongoing efforts to expand and enhance existing FEMA-356 guidelines (such as the ATC-58 effort) or to develop an entirely new methodology (such as the collaborative effort within the Pacific Earthquake Engineering Research (PEER) center). Though there are intrinsic differences in the various methods, they all share some common elements that are outlined below.

### **1. Performance Objectives**

A performance objective may be regarded as the first element in PBSD and is composed of two parts: a performance level and a hazard level which describes the expected seismic load at the site. Terms such as Collapse Prevention (CP) and Life Safety (LS) are examples of performance levels. In the probabilistic format of the PEER methodology, a decision variable (such as dollar loss or downtime) is used to quantify the performance objective. Hazard levels are typically prescribed in terms of response spectra and are controlled by site characteristics. If time histories are used to evaluate the performance of a building, then the selected records must possess characteristics (including source mechanism and fault

distance) equivalent to those that control the design spectra. FEMA-356 specifies the following three hazard levels:

- *Hazard Level I (Service Level Earthquake)* – A relatively frequent earthquake with a 50% probability of being exceeded in 50 years.
- *Hazard Level II (Design Level Earthquake)* – Earthquakes at this level of hazard are normally assumed to have a 10% probability of being exceeded in 50 years.
- *Hazard Level III (or a Maximum Credible Level Earthquake)* – The maximum credible event at the site with a 2% probability of being exceeded in 50 years.

## **2. Demand Prediction**

The next step in a performance-based evaluation is the estimation of seismic demands in both structural and non-structural elements in the structure due to the imposed earthquake loads. The prediction of deformation demands is arguably the most critical step in PBSB. Determining demands necessitates the development of a structural model of reasonable complexity. Errors in estimating the demand as a result of an inadequate structural model can propagate through and lead to misleading conclusions on the performance of the structure. FEMA-356, for example, prescribes four different analytical procedures to estimate demands in a building. This paper is concerned primarily with non-linear procedures and the differences between static and dynamic methods to estimate seismic demands.

## **3. Performance Assessment**

In this third and final phase of the procedure, the seismic demands computed in the previous step are compared with acceptable levels of damage for various performance states. Performance measures are typically derived from experimental evidence which quantify a damage state with a demand value. Though this paper is not concerned with acceptance criteria, findings from the study shed light on the conceptual basis for developing such criteria when using non-linear analysis procedures.

## **4. Establishing Seismic Demands Using Non-linear Procedures**

It becomes evident from the three elements of PBD outlined above that the determination of seismic demands is a critical step in the overall process. Demands can be evaluated using linear or non-linear procedures. FEMA-356, for example, lists four different analytical methods to evaluate demands. Since seismic forces at the design event are expected to result in non-linear structural behavior, it is reasonable to expect non-linear procedures to be used in calculating element deformation demands. Of the two non-linear methods, static procedures involving pushover analyses are obviously going to be favored over time-history procedures by design practitioners. Hence, the focus of this study revolves around the consequence of using pushover methods in seismic demand estimation.

Early literature predating FEMA-356 on non-linear lateral load analysis include the work of Freeman (1978), Fajfar and Fischinger (1988), and Eberhard and Sozen (1993). Since the publication of FEMA-356, pushover methods have been the subject of several investigative studies (Krawinkler and Seneviratna, 1998; Tso and Moghadam, 1998; Satyarno et al., 1998; Wight et al., 1999; Mwafy and Elnashai, 2001). Studies by Kunnath and Gupta (2000) and Kunnath and John (2000) have investigated different lateral load patterns recommended in FEMA-356 and identified inconsistencies in the different pushover procedures currently in use. Previously, Iwan (1999) demonstrated the inability of pushover methods to predict demands for pulse-like near fault ground motions. A well-known issue with a pushover analysis using standard lateral load configurations (such as an inverted triangular or a uniform distribution) is that it fails to account for certain critical higher mode contributions. The drawbacks in pushover methods using invariant FEMA-based lateral load patterns have led to alternative pushover strategies. The multi-mode pushover (Sasaki et al., 1998) tries to incorporate higher modes by considering multiple pushover curves derived from different modal force patterns. The Adaptive Pushover Method, developed by Gupta and Kunnath (2000), uses a varying load pattern that pushes and pulls the structure by combining modes at different stiffness states of the structure. More recently, Chopra and Goel (2002) proposed a modal pushover technique that combines the response of individual modal demands (though only the first few modes are typically needed) with reasonable success.

### 5. Objectives and Scope of Study

The objective of this study stems from the rapid popularity of pushover analysis in engineering practice facilitated in large part by the availability of non-linear static procedures in commercial software such as SAP2000 (Computers and Structures, 2003). While non-linear procedures do represent a significant advance in the current state-of-the-practice in seismic design, it is important to recognize and document the inherent limitations in pushover methods. Ultimately, the objective of a seismic evaluation is to identify deformation demands in structural components during an earthquake and whether these demands will exceed the capacity of the element. Traditional design practice (using *R*-factors) examines the overall response of the system in terms of base shear and roof displacement implying that local demands are controlled by global demands. The advent of pushover procedures facilitates the estimation of demand at both global and local levels, thereby providing a means of validating this assumption. But a pushover procedure is a static method. Hence, in the first part of this paper, non-linear static responses are compared with non-linear time-history analyses to ascertain the validity of using static methods to compute dynamic demands. The comparison is carried out for inter-story drift demands and local component demands. More importantly, three different lateral load configurations suggested in FEMA-356 are used for the pushover analyses. This is followed by a more detailed examination of local deformation demands and the implications of cumulative damage resulting from cyclic loading. The study is limited to regular medium-rise moment frame buildings.

### DESCRIPTION OF BUILDINGS USED IN EVALUATION

The findings reported in this study are based on non-linear static and dynamic analysis of steel and reinforced concrete moment frame buildings. Both designs are based on configurations presented in the SEAOC Seismic Design Manual (SEAOC, 2000). The original design of the steel frame presented in the manual pertains to a four-story building. In this study, the same floor plan is extended to eight and twelve stories. The concrete building in the original SEAOC manual is a seven-story structure. Here, the same building plan is used to develop designs for eight- and twelve-story buildings. The designs satisfy the minimum requirements of the Uniform Building Code, which contain provisions for limiting inter-story drift and ensuring a strong-column weak-beam connection. No enhanced provisions (such as the principles of capacity design used in New Zealand) are incorporated in the final designs.

#### 1. Steel Buildings

The floor plan of the building is shown in Figure 1. There are 7 bays in the EW direction and 5 bays in the NS direction of the building covering a total plan of 55.8 m by 37.5 m. The first floor is 4.5 m high and the remaining floor heights are 4.1 m. Member sizes for both the 8-story and 12-story frames are provided in Table 1.

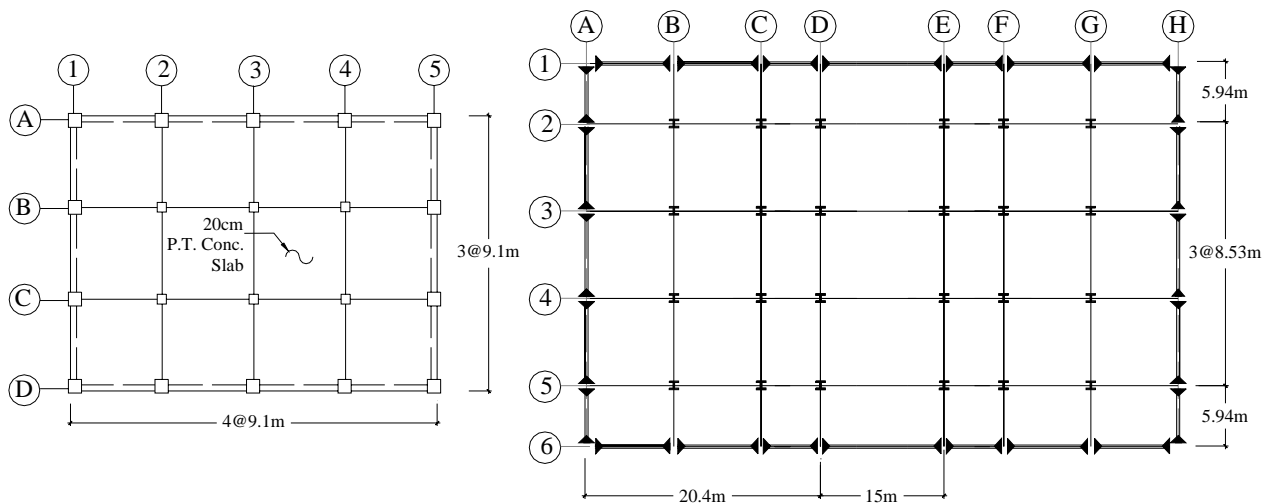


Fig. 1 Plan view of RC building (left) and steel structure (right)

**Table 1: Member Details of Steel Frame along Line A**

8-Story Steel			12-Story Steel		
Levels	Beam Section	Column Section	Levels	Beam Section	Column Section
7 – 8	W21x73	W14x132	11 – 12	W27x94	W14x132
5 – 6	W24x94	W14x159	9 – 10	W27x102	W14x193
3 – 4	W27x102	W14x211	7 – 8	W27x114	W14x257
1 – 2	W27x114	W14x283	5 – 6	W30x124	W14x311
			3 – 4	W30x132	W14x370
			1 – 2	W30x148	W14x426

The lateral force resisting system in each case is a perimeter moment frame. The interior frames are designed to carry gravity loads and are pinned at the base. Exterior frames columns are supported on piles and they are assumed to be fixed at the ground level. The design of the building is based on the requirements of the 1997 UBC provisions. The design roof dead load is 9194 kN (2066 kips) and the dead load of each floor is 9945 kN (2235 kips). The yield strength of steel is assumed to be 344.75 MPa (50 ksi) for all structural members of the building. The design base shear for both the 8- and 12-story structures is approximately 4.8% of their respective building weights.

## 2. Concrete Moment Frame Buildings

The plan and elevation of a typical frame is displayed in Figure 1. Only a typical frame in the long (EW) direction along line A (Figure 1) is evaluated in this study. Section properties of the beams and columns that constitute this frame are itemized in Table 2 for both the 8-story and 12-story structures. Each bay in both directions span approximately 9.1 m (30 ft). The height of the first floor is 4.3 m, while the remaining floors are 3.66 m each. The roof weight of the building is based on a uniformly distributed load of 7.55 kN/m<sup>2</sup> and typical floor weights are determined from 8.9 kN/m<sup>2</sup>. Like the steel building, each frame in the RC structure is designed to UBC 97 standards for Seismic Zone 4, standard occupancy, Seismic Source Type A (capable of high-magnitude frequent events), and UBC soil profile type S<sub>D</sub> (stiff soil with a shear wave velocity between 183 m/s and 365 m/s).

## DEVELOPMENT OF BUILDING MODELS

Since both structures are essentially symmetric, it was necessary to model only a typical two-dimensional frame without affecting the outcome of the study. Two-dimensional computer models of each building frame were developed for use with OpenSees (2003). The current version of OpenSees includes a general model-builder for creating two- and three-dimensional frame and continuum models using a scripting language called TCL. A typical frame is modeled as a two-dimensional framework of beams and columns. Beams and columns are modeled using force-based non-linear beam column elements that consider the spread of plasticity along the length of the element. The integration along the element is based on Gauss-Lobatto quadrature rule. A fiber section model at each integration point, which in turn is associated with uniaxial material models and enforces the Bernoulli beam assumption for axial force and bending, represents the force-based element. Centerline dimensions were used in the element modeling for all cases. For the time-history evaluations, one half of the total building mass was applied to the frame distributed proportionally to the floor nodes.

The evaluation of the steel buildings is based on the response of a typical perimeter frame in the north-south direction. As indicated in Figure 1, this frame consists of 5 bays with two exterior spans of 5.94 m and three interior spans of 8.53 m. Each beam section is discretized into a series of fibers whose stress-strain response is represented by a bilinear model with an elastic slope of 200 GPa and a post-yield strain-hardening ratio of 2%. Axial-flexure interaction is included in both the beams and columns. The composite action of floor slabs was not considered.

Here, a typical frame in the east-west direction was considered. Cross-sectional properties for the fiber model are specified for each member in terms of a mesh of concrete fibers and discrete reinforcing bars. The uniaxial properties for non-linear modeling of the concrete fibers are shown in Figure 2. The rebar is modeled as Grade 60 steel (yield strength of 414 MPa) with an ultimate strength of 620 MPa and Young's Modulus of 200 GPa. The non-linear material behavior is modeled as a bilinear curve with post-yield strain-hardening ratio of 2%.

**Table 2: Section Details of Exterior Concrete Frame along Line A**

Levels	Exterior Columns		Interior Columns		Beams			
	Size *	Steel **	Size *	Steel **	Size *	Top Steel **	Bottom Steel **	
8-Story RC	1	101x101	20-#11	112x91.5	18-#11	107x66	5 #11+5#4	5 #9+5#4
	2	101x101	20-#9	112x91.5	18-#10	112x66	5 #11+5#4	5 #10+5#4
	3	101x101	20-#9	112x91.5	18-#10	107x66	5 #11+5#4	5 #10+5#4
	4	96.5x96.5	20-#9	107x86	18-#10	107x66	5 #11+5#4	5 #10+5#4
	5	96.5x96.5	20-#9	107x86	18-#10	96.5x66	5 #11	5 #9
	6	91.5x91.5	16-#9	107x86	16-#10	91.5x61	5 #10	5 #8
	7	91.5x91.5	16-#9	96.5x76	16-#8	86x61	5 #10	5 #7
	8	91.5x91.5	16-#10	96.5x76	16-#8	86x61	5 #9	5 #7
12-Story RC	1	86x86	24-#11	107x81	18-#14	112x71	6 #11+5#4	6 #10+5#4
	2	81x81	20-#10	107x81	18-#14	112x71	7 #11+5#4	6 #10+5#4
	3	81x81	20-#10	107x81	18-#14	107x66	6 #11+5#4	6 #10+5#4
	4	81x81	20-#10	107x81	18-#11	107x66	6 #11+5#4	6 #10+5#4
	5	79x79	20-#10	107x81	18-#11	107x66	6 #11+4#4	6 #10+4#4
	6	79x79	20-#10	107x81	18-#11	107x66	6 #11+4#4	5 #10+4#4
	7	79x79	20-#10	96.5x76	18-#11	107x66	6 #11+4#4	5 #10+4#4
	8	76x76	20-#9	96.5x76	18-#11	107x66	5 #11+4#4	5 #10+4#4
	9	76x76	20-#9	96.5x76	18-#10	96.5x66	5 #11	5 #9
	10	71x71	16-#9	86x71	18-#10	91.5x61	5 #11	5 #8
	11	71x71	16-#9	81x61	16-#9	86x61	5 #10	5 #7
	12	71x71	16-#8	81x61	16-#9	81x61	5 #9	4 #7

\* All dimensions are in cm

\*\* Number of bars-diameter => #4: 13mm; #5: 16mm; #6: 19mm; #7: 22mm; #8: 25mm; #9: 29mm; #10: 32mm; #11: 35mm

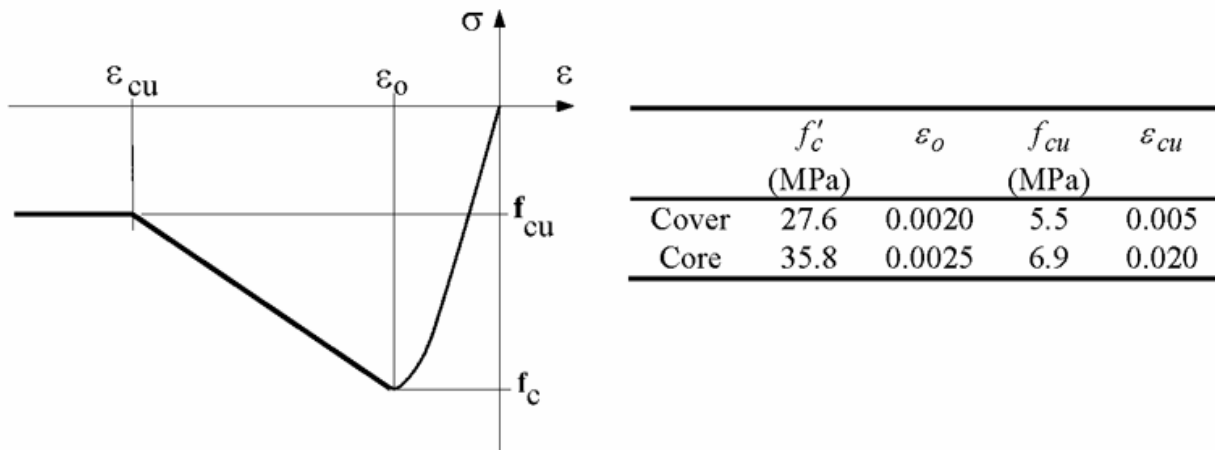


Fig. 2 Concrete material model

As in the case of the steel structure, the concrete building was modeled as a bare frame without considering the contribution or interaction of the floor slab. Clearly, the contribution of the slab on both the stiffness and strength of the beam is well established; however, these effects are not expected to influence the findings in this study since the same models are being used in the different analyses.

**COMPARATIVE STUDY OF SEISMIC DEMANDS**

The four buildings described in the previous section are evaluated using non-linear static and non-linear dynamic procedures to compare the resulting demands. In the case of static approaches, the following lateral load configurations were considered:

*NSP-1*: The buildings are subjected to a lateral load distributed across the height of the building based on the following equation:

$$F_x = \frac{W_x h_x^k}{\sum W_x h_x^k} V \quad (1)$$

In the above expression,  $F_x$  is the applied lateral force at level 'x',  $W$  is the story weight,  $h$  is the story height, and  $V$  is the design base shear. This results in an inverted triangular distribution of the lateral load when the period-dependent power  $k$  is set equal to unity.

*NSP-2*: A uniform lateral load distribution consisting of forces that are proportional to the story masses at each story level.

*NSP-3*: A lateral load distribution that is proportional to the story shear distribution determined by combining modal responses from a response spectrum analysis of each building model using the BSE-2 hazard spectrum as recommended in FEMA-356.

### 1. Target Displacement

Each of the four building models were subjected to the three lateral load patterns enumerated above until the roof reached a specified target displacement. The target displacements were computed using the provisions in FEMA-356 for BSE-2 loading. A site-specific spectrum was developed using the following parameters to characterize a hazard level corresponding to the maximum credible earthquake (or Hazard Level III):  $S_s = 2.0$ ;  $S_1 = 0.75$ ;  $F_a = 1.0$ ;  $F_v = 1.5$ ; Site Category D and 5% damping. Assuming  $\beta_s = 1$ ,  $\beta_1 = 1$ , the following ranges of spectral acceleration values were obtained:

$$\text{for } 0 < T < T_0: S_a = 10.67 T + 0.8$$

$$\text{for } T_0 < T < T_s: S_a = 2.0$$

$$\text{for } T > T_s: S_a = 1.125/T$$

In the above expressions,  $T_s = 0.5625$  s, and  $T_0 = 0.1125$  s. This resulted in the following values of target displacements:

Steel frame: 8-story = 1.08 m; 12-story = 1.30 m.

RC frame: 8-story = 0.40 m; 12-story = 0.54 m.

The BSE-2 design spectrum, developed using the parameters above, are superimposed on the earthquake spectra shown in Figure 3. The fundamental periods of each building model are also identified in these figures.

**Table 3: Ground Motion Details**

EQ. No	Year	Earthquake	Recording Station	PGA (g)	Distance (km) *	EQ. Scale Factor †			
						8-Story Steel	12-Story Steel	8-Story RC	12-Story RC
1	1971	San Fernando	Station 241	0.25	16.5	3.7	3.5	4.3	3.5
2	1971	San Fernando	Station 458	0.12	18.3	3.5	3.0	5.9	4.1
3	1989	Loma Prieta	Hollister, South & Pine	0.18	17.2	3.8	3.5	4.1	4.7
4	1989	Loma Prieta	Gilroy #2	0.32	4.5	6.1	6.8	3.0	2.6
5	1992	Landers	Yermo	0.15	31.0	5.3	5.4	5.5	4.5
6	1992	Landers	Joshua Park	0.28	10.0	3.9	5.0	3.4	2.8
7	1994	Northridge	Century City LACC North	0.26	23.7	5.5	6.0	6.7	6.7

\* Closest distance to fault; † Scale factor used to achieve the target roof displacement

### 2. Benchmark Demands: Time History Analyses

The validity of pushover procedures based on the three invariant load distributions is examined using the results of non-linear time-history analyses as a benchmark. A set of seven strong ground motions, all recorded at soil sites in California and having a magnitude range of 6.6 to 7.5 were selected for the non-linear time-history evaluations. These ground motion records are recommended by ATC-40 (ATC, 1996). Details of these records are given in Table 3, and their five-percent damped elastic acceleration response spectra are shown in Figure 3 for each set of building evaluations. To facilitate the comparison with pushover analyses, the selected ground motions are scaled in such a manner so that the resulting peak roof

displacement is equal to the target displacement computed for each building. The scale factors are also listed in Table 3. A conventional technique is to scale ground motions such that the spectral acceleration at the fundamental period matches a given design spectrum. The scaling method adopted in this study is based on the FEMA recommended guideline for the expected peak roof displacement. Though the scale factors appear to be quite high in some cases, the spectral acceleration at the fundamental period of the respective structural models is comparable to the BSE-2 spectrum for the steel buildings and somewhat higher than the BSE-2 spectrum for the RC structures.

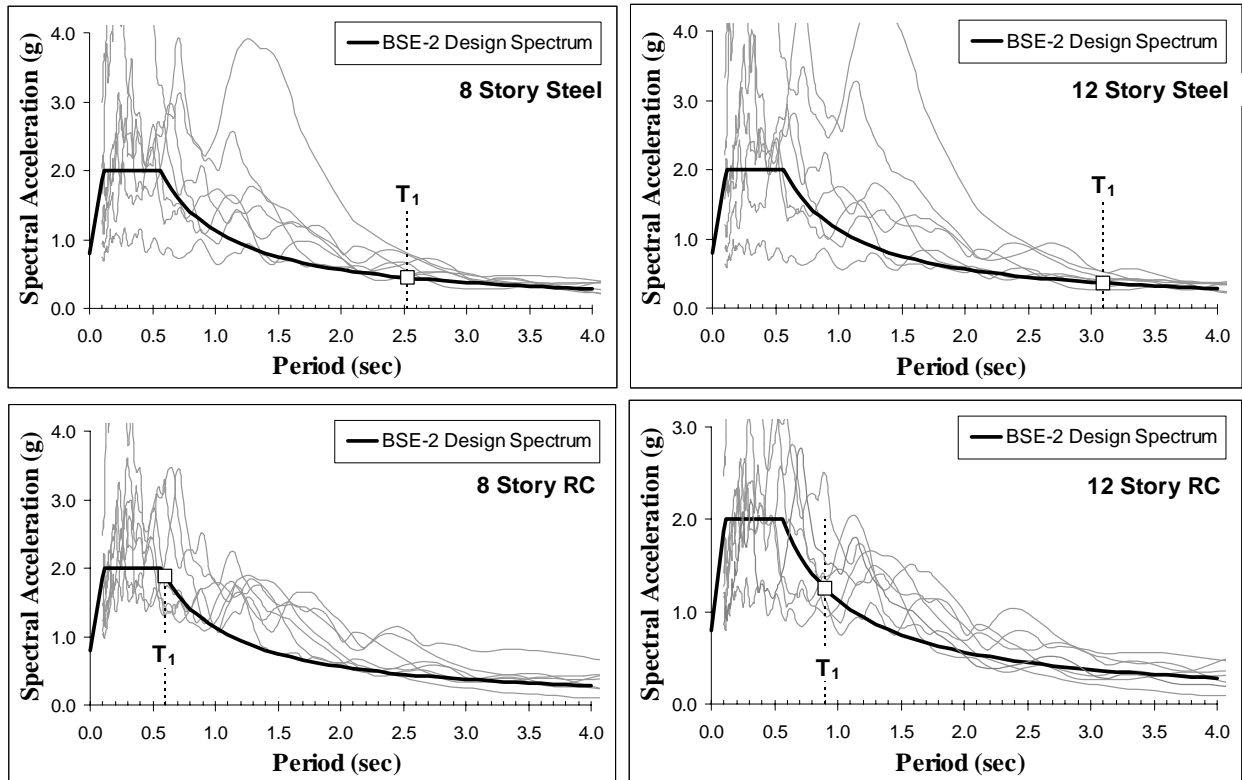


Fig. 3 Spectra of scaled ground motion recordings used in the evaluation of each building

### 3. Evaluation of Seismic Demands

The estimated demands using the different non-linear procedures are evaluated at the global, story and local levels. Global demands refer to the displacement profile of the building at the peak roof displacement and the base shear versus roof displacement response. At the story level, the inter-story drift values are compared. Finally, local demands are evaluated in terms of inelastic rotations at the ends of beam and column elements. Collectively, these deformation measures provide a basis for comparing the effectiveness of static pushover methods to predict demands resulting from seismic action.

#### 3.1 Global Demands

Estimates of global demand from the non-linear time-history (NTH) analyses for both steel and concrete structures are shown in Figures 4(a) through 7(a). The magnitudes at each story for each record (listed as Eq-1 through Eq-7) correspond to the maximum demand at that story throughout the duration of the event. The mean and the distribution around the mean value are repeated in Figures 4(b) through 7(b) to enable direct comparison with demands estimated from the pushover procedure using the three lateral load patterns. Recall that ground motions were scaled to produce the same target roof displacement. In all cases, the inverted triangular pattern is found to come closest to the mean time-history estimates. The other two load patterns tend to overestimate demands at the lower levels because these patterns typically result in higher loads being applied at the lower floors.

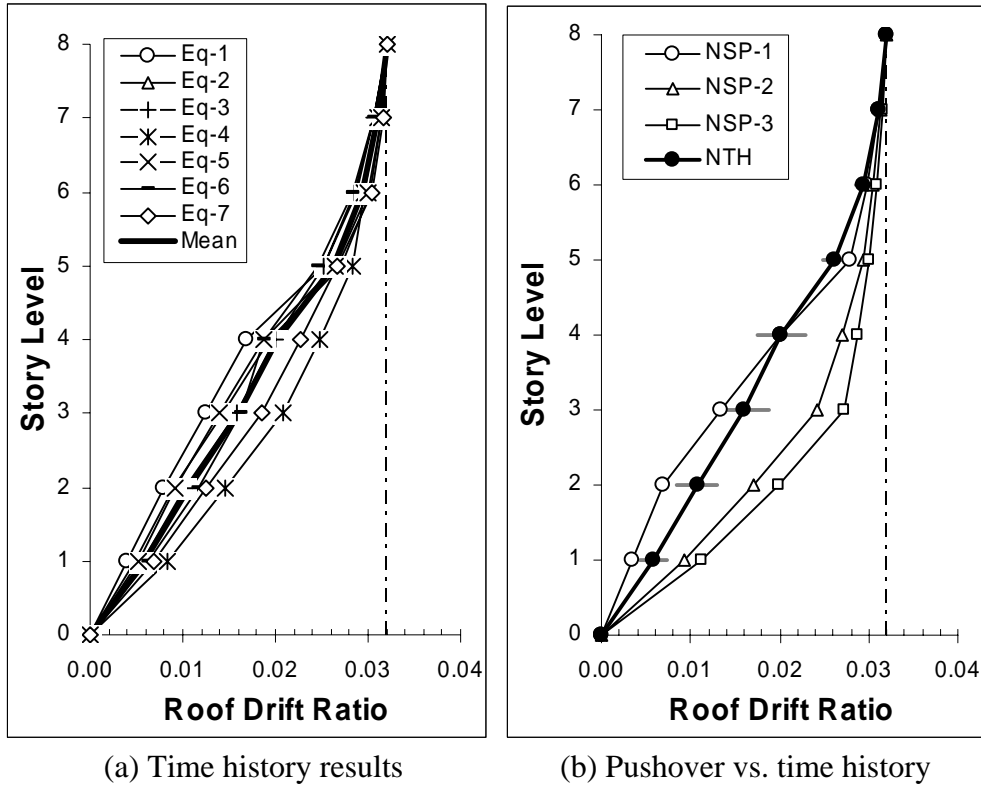


Fig. 4 Peak displacement profiles for 8-story steel frame under static and seismic loads (Note: Horizontal band across NTH estimate shows distribution of peak demands across the mean value)

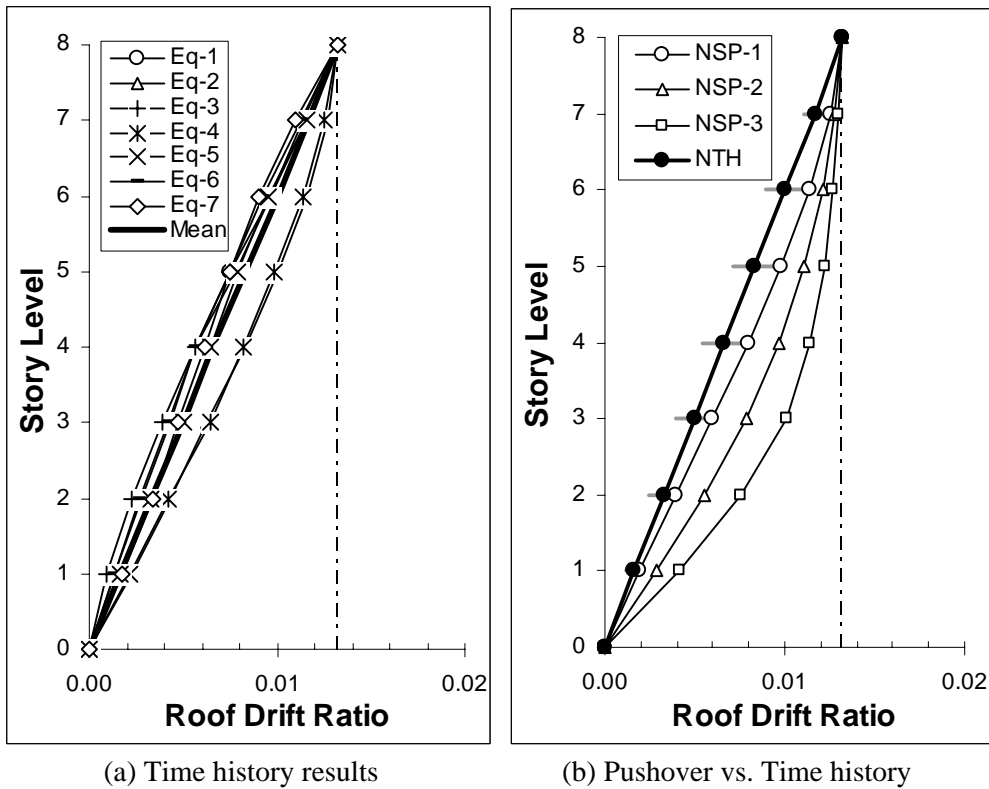


Fig. 5 Peak displacement profiles for 8-story RC frame



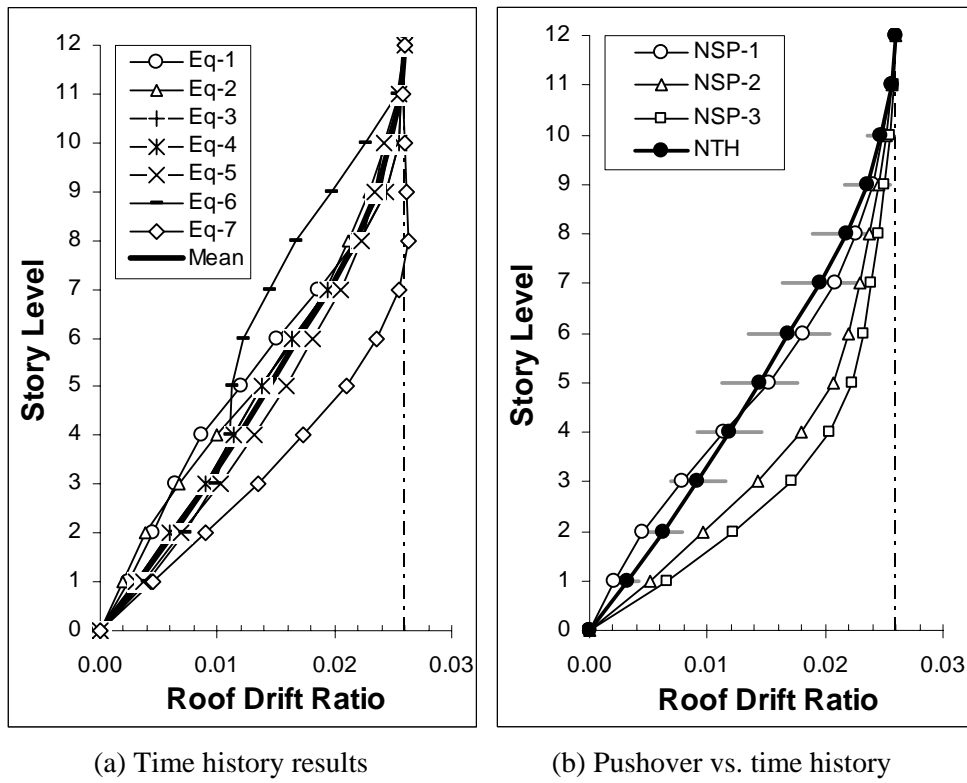


Fig. 6 Peak displacement profiles for 12-story steel frame

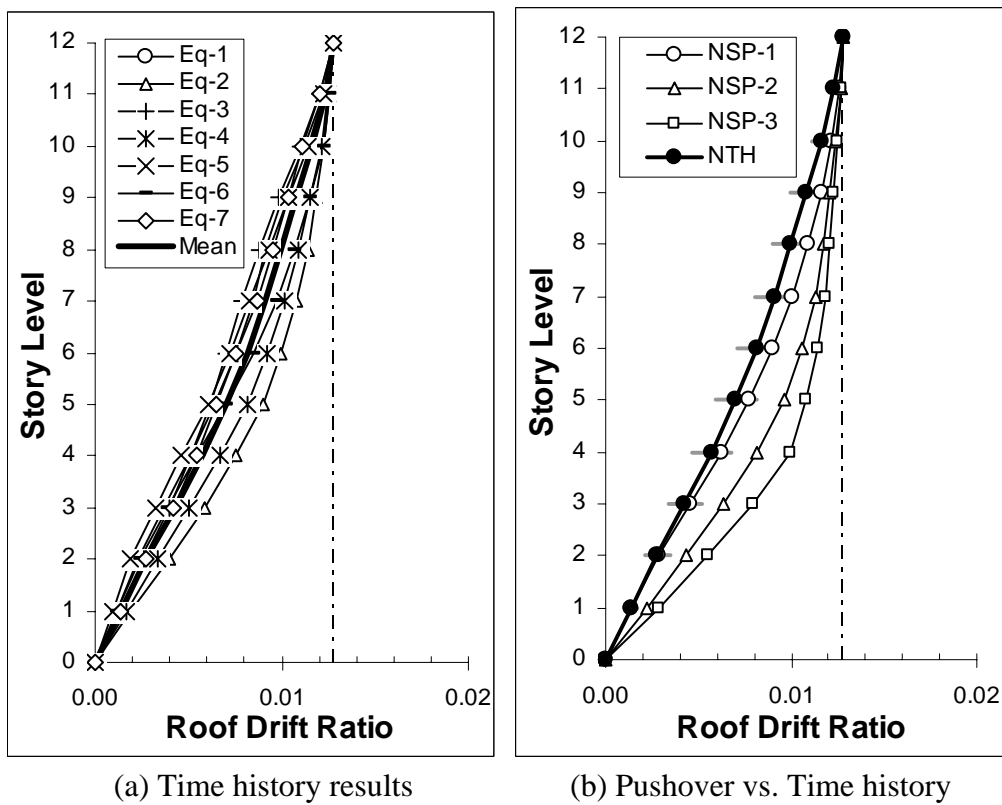
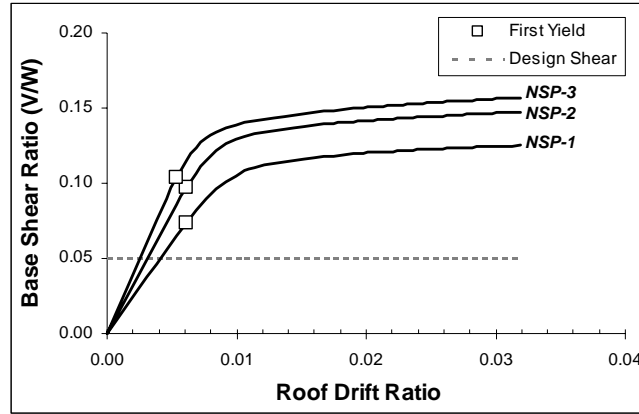
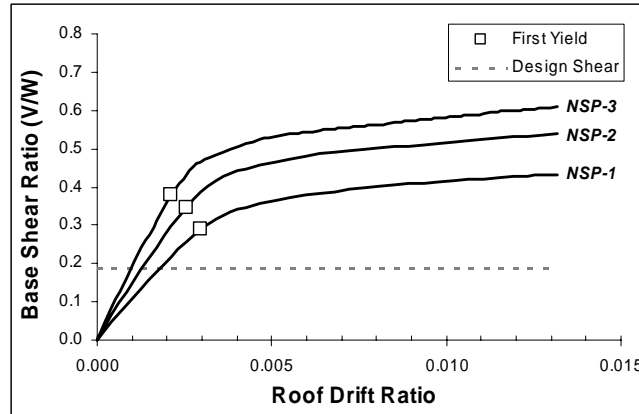


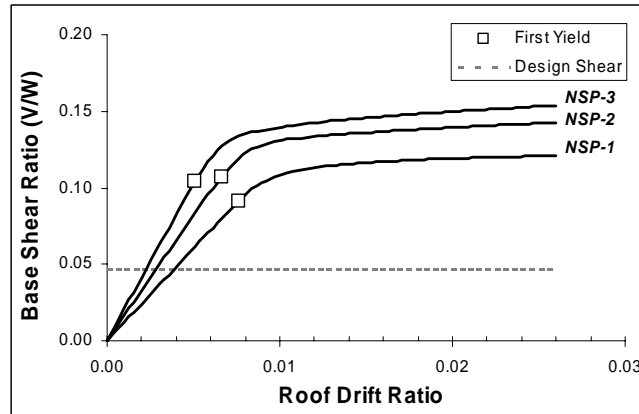
Fig. 7 Maximum displacement profiles for 12-story RC frame



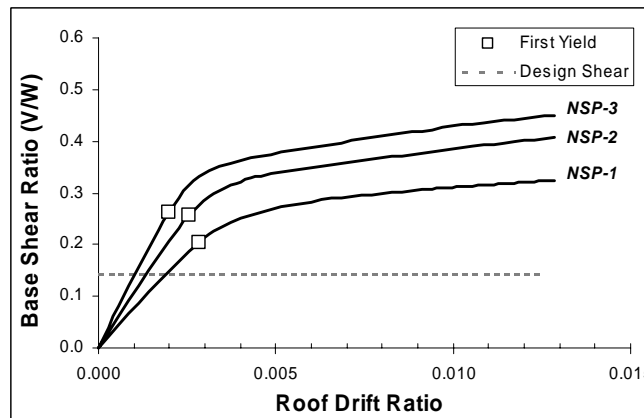
(a) 8-story steel building



(b) 8-story RC building

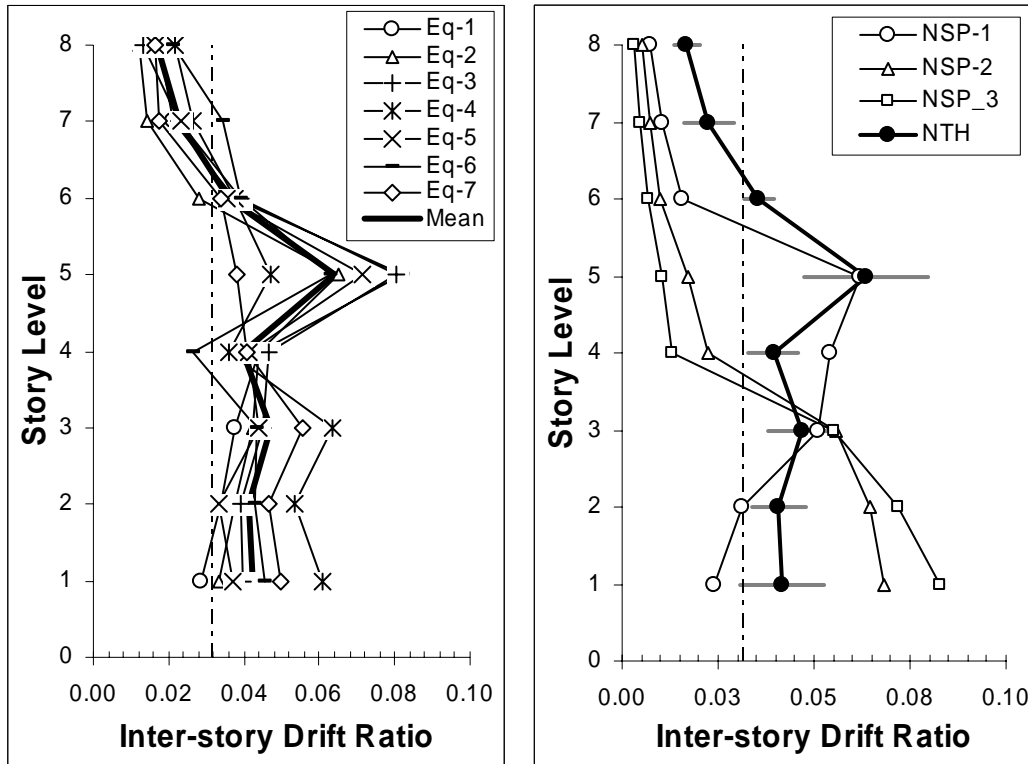


(c) 12-story steel building



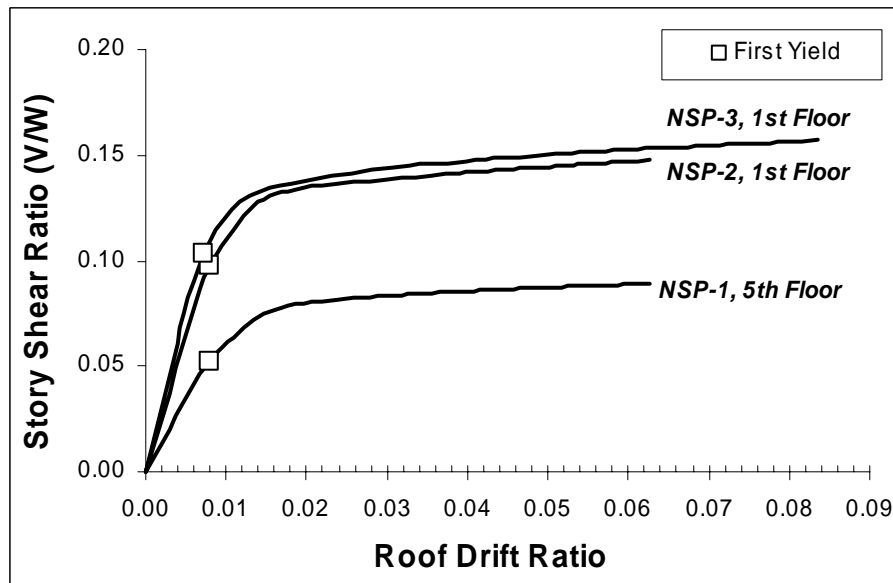
(d) 12-story RC building

Fig. 8 Base shear vs. roof drift response using different lateral load profiles



(a) Time history results

(b) Pushover vs. time history



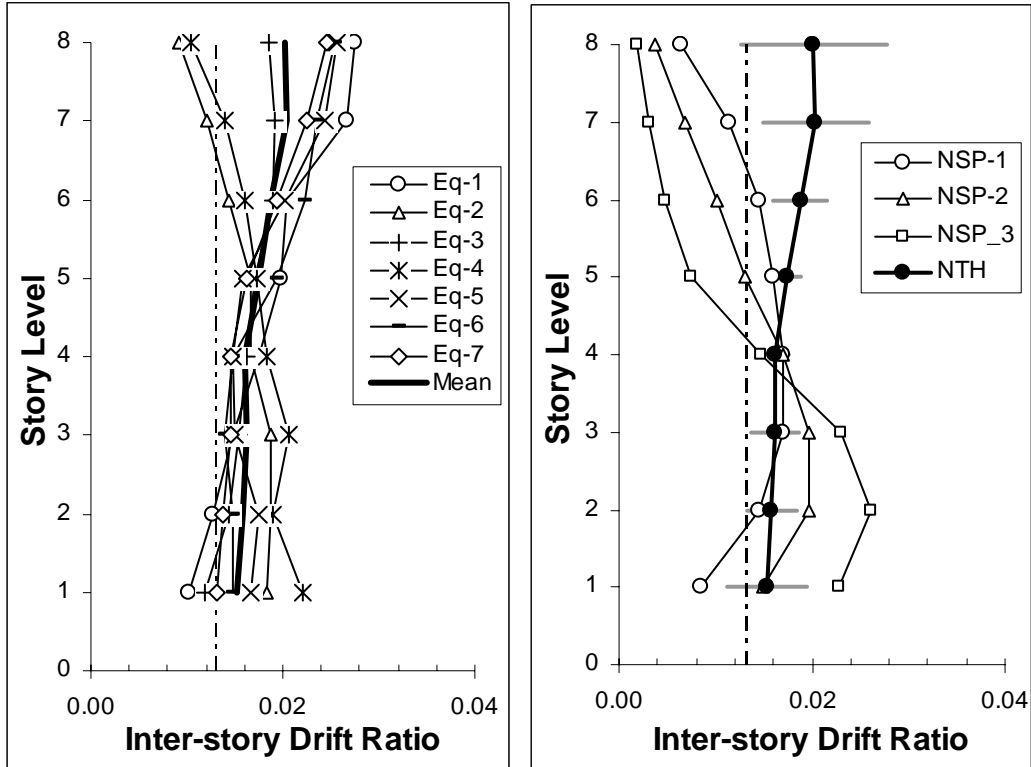
(c) Typical capacity curves for critical stories

Fig. 9 Inter-story demands in 8-story steel frame

The capacity curves which show the total base shear (in terms of the building weight) as a function of the roof drift is displayed in Figure 8 for all models. Initial yielding of an element occurs first when using NSP-1. This loading pattern also produces a response with the least system stiffness and the lowest base shear capacity. However, the difference in base shear capacity between the different patterns decreases with story height. The difference is more evident for the steel building since the increase in story height produced a larger change in fundamental period than the RC building. The design base shear for each building is identified in these plots for comparison.

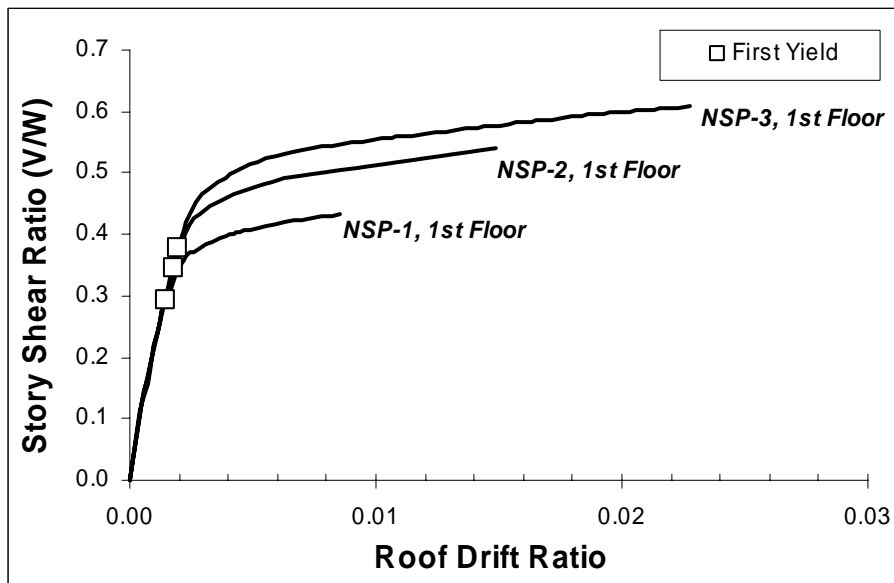
The information generated in Figures 4 through 8 represents the fundamental measures of demand at the global level. The inherent ductility of the system is typically evaluated using the response shown in Figure 8. This plot contains two elements of the reduction or *R*-factor used in modern building codes: the

difference between first yield of an element and eventual yield of the system contains information on the redundancy in the system while the response beyond system yield up to the target deformation is a measure of the ductility-based reduction factor. The question that this paper attempts to address is whether these measures are adequate to reach an assessment of the performance of the building. In the next section, additional demand measures are evaluated using the information from non-linear time-history analyses as benchmark estimates.



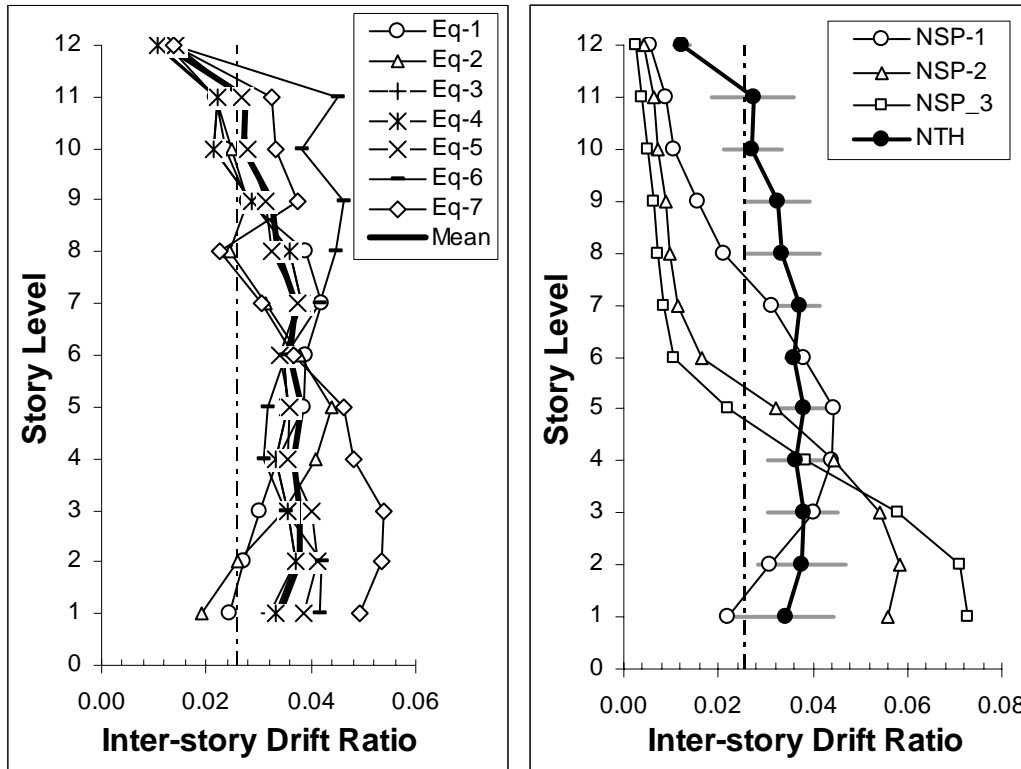
(a) Time history results

(b) Pushover vs. time history



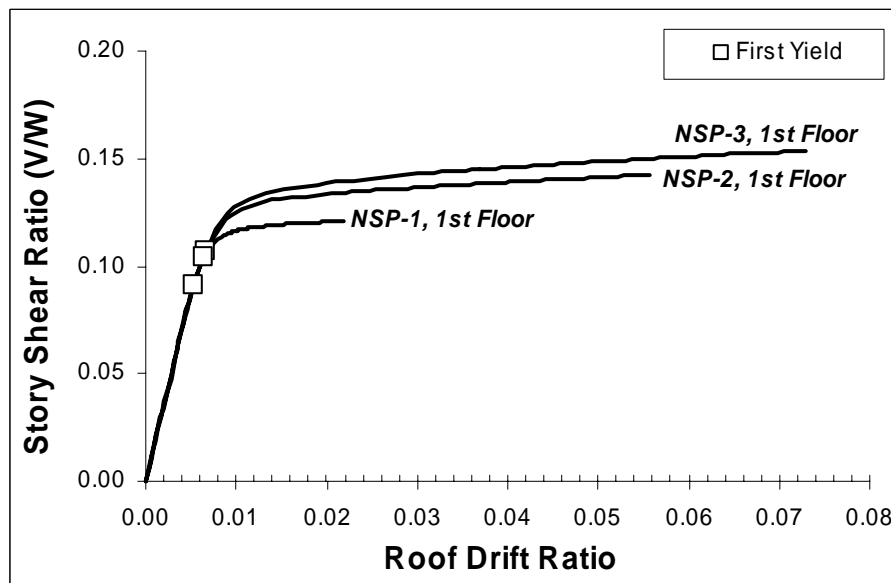
(c) Typical capacity curves for critical stories

Fig. 10 Inter-story demands in 8-story RC frame



(a) Time history results

(b) Pushover vs. time history



(c) Typical capacity curves for critical stories

Fig. 11 Inter-story demands in 12-story steel frame

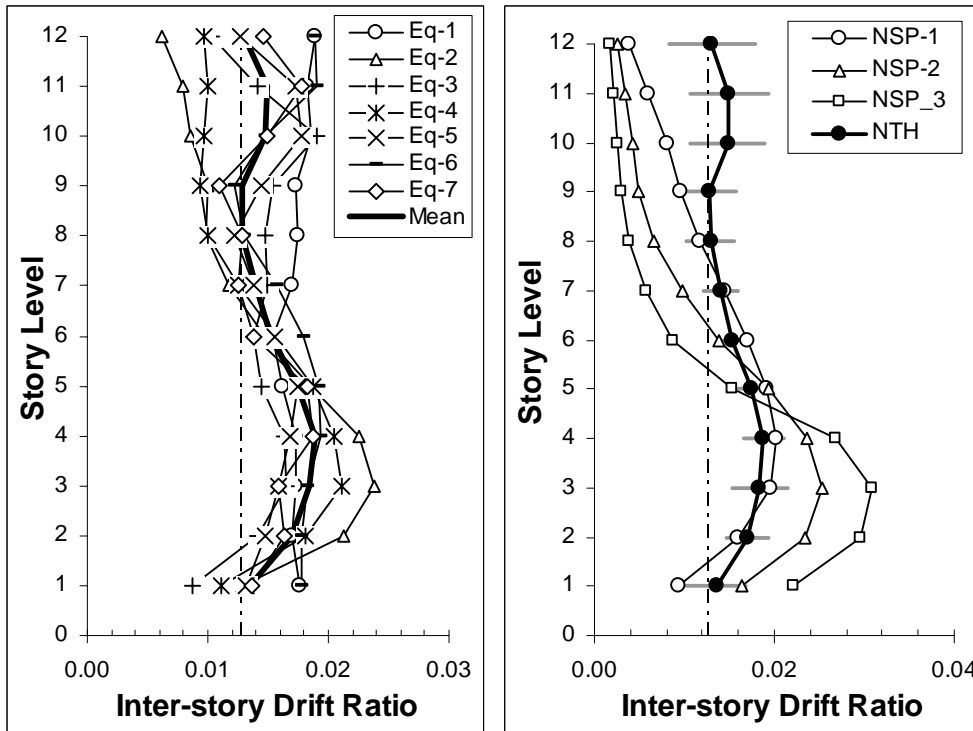
### 3.2 Story Level Demands

The importance of inter-story drift has long been recognized as an important indicator of building performance. During an earthquake, the inter-story displacements vary with time as different modes dominate the response. On the other hand, pushover methods, which use invariant load patterns, produce a consistent pattern of inter-story demands up to initial yielding following which the story demands become localized and depend on the story level to experience first excursion beyond the elastic state.

Inter-story demands are plotted in Figures 9-12 for the four building models evaluated in this study. In each case, demands are shown for each earthquake followed by a plot which compares time-history

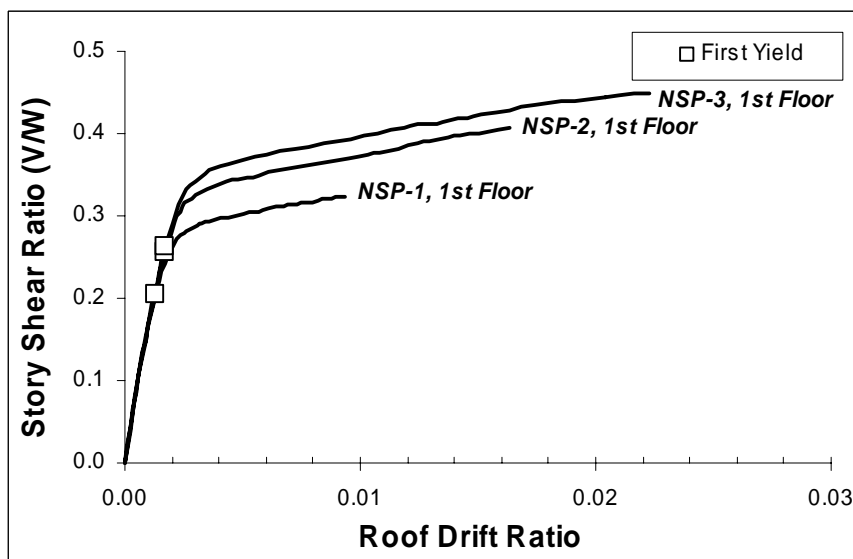
estimates with pushover demands. The third plot for each frame shows capacity curves for critical story levels (which are defined as those stories that exhibit the largest inter-story drift demands).

The most important observation that results from the non-linear time-history evaluation is that the peak story demands vary from one record to the next. While several earthquakes impose the largest demand at the lower levels, there are a number of cases when the largest demands occur at different levels. In general, pushover methods tend to over-estimate the story demands at the lower levels and under-estimate them at the upper levels. The discrepancy becomes more apparent with increasing story height (or longer fundamental periods). Story capacity curves that result from pushover procedures serve to reinforce the finding that static methods cannot adequately reproduce demands across the height of the building when compared to typical responses using non-linear time-history analyses.



(a) Time history results

(b) Pushover vs. time history



(c) Typical capacity curves for critical stories

Fig. 12 Inter-story demands in 12-story RC frame

### 3.3 Local Element Demands

In the third and final phase of the evaluation, demands are examined at the element level. Since story demands reflect the behavior of elements at that story, it is reasonable to expect local element demands to correlate to story demands. Based on the story drifts and story capacity curves presented in Figures 11 and 12, the ductility demands at critical story levels are summarized in Tables 4 and 5. The tables include measures at the global level and at the component level. Only a set of selected stories and elements at these story levels experiencing the maximum demands are shown. In addition to the estimates computed for the different lateral load patterns using pushover analysis, the peak ductility demands resulting from the critical earthquake record (causing the largest demands) is also displayed. In the case of the 8-story steel structure, local component demands are generally much higher than story demands with column demands exceeding beam ductility demands.

**Table 4: Summary of Ductility Demands for Steel Buildings**

<b>8-Story Steel</b>						
		<b>NSP-1</b>	<b>NSP-2</b>	<b>NSP-3</b>	<b>(NTH, EQ-5)</b>	<b>(NTH, Mean)</b>
<b>Global</b>		5.3	5.3	6.0	-	-
<b>Story-1</b>	<b>Story</b>	3.7	7.8	11.7	-	-
	<b>Interior Column</b>	4.8	14.3	17.2	6.8	8.5
	<b>Exterior Beam</b>	4.6	11.6	13.5	5.8	7.1
<b>Story-3</b>	<b>Story</b>	5.0	5.7	6.1	-	-
	<b>Interior Column</b>	16.9	19.7	19.7	8.9	7.5
	<b>Exterior Beam</b>	9.3	4.7	4.7	8.2	6.8
<b>Story-5</b>	<b>Story</b>	7.8	2.4	6.7	-	-
	<b>Interior Column</b>	17.0	5.5	5.5	22.0	16.9
	<b>Exterior Beam</b>	2.5	1.2	1.3	7.1	5.9

<b>12-Story Steel</b>							
		<b>NSP-1</b>	<b>NSP-2</b>	<b>NSP-3</b>	<b>(NTH, EQ-6)</b>	<b>(NTH, EQ-7)</b>	<b>(NTH, Mean)</b>
<b>Global</b>		3.4	3.9	5.1	-	-	-
<b>Story-1</b>	<b>Story</b>	4.1	8.4	11.5	-	-	-
	<b>Interior Column</b>	4.8	12.2	15.1	7.1	9.6	7.2
	<b>Exterior Beam</b>	5.0	11.2	14.4	7.8	10.0	7.1
<b>Story-3</b>	<b>Story</b>	4.8	6.4	7.1	-	-	-
	<b>Interior Column</b>	3.8	3.0	4.8	4.9	3.4	2.6
	<b>Exterior Beam</b>	8.3	9.9	9.1	8.5	10.2	6.3
<b>Story-5</b>	<b>Story</b>	4.9	3.5	2.4	-	-	-
	<b>Interior Column</b>	3.1	4.8	3.4	5.12	5.5	3.7
	<b>Exterior Beam</b>	8.0	3.9	2.7	9.4	7.6	5.7
<b>Story-9</b>	<b>Story</b>	1.5	0.0	0.0	-	-	-
	<b>Interior Column</b>	2.0	0.0	0.0	6.3	5.5	4.4
	<b>Exterior Beam</b>	1.7	0.0	0.0	10.0	6.8	5.4

NTH = Nonlinear Time History

The response using time-history analyses produced smaller demands at lower stories of the 8-story buildings but caused higher peak column demands at the critical fifth story level. Similarly, no correlation between global, story and local element demands are evident for the 12-story steel frame. Findings from the steel buildings also apply to the response results obtained for the RC structures, as indicated in the data presented in Table 5. The component demands at the upper floors of the 12-story buildings support the conclusions reached when examining story levels demands which show pushover methods severely under-predicting deformations and the potential for yielding at these floors.

Table 5: Summary of Ductility Demands for RC Buildings

		8-Story RC									
		NSP-1		NSP-2		NSP-3		(NTH, EQ-1)		(NTH, Mean)	
	<b>Global</b>		4.4		5.2	-	6.2		-		
Story-1	<b>Story</b>		5.8		8.3		11.6		-	-	
	<b>Column</b>	Ext.	6.5	Ext.	9.5	Ext.	12.4	Ext.	4.5	Ext.	5.2
	<b>Beam</b>	Ext.	7.7	Ext.	10.7	Ext.	12.9	Ext.	5.2	Ext.	4.5
Story-3	<b>Story</b>		5.0		5.1		5.1		-	-	
	<b>Column</b>	Ext.	1.2	Int.	2.5	Int.	3.6	Ext.	2.2	Ext.	2.2
	<b>Beam</b>	Int.	6.3	Int.	7.2	Ext.	7.2	Ext.	4.9	Ext.	5.1
Story-5	<b>Story</b>		4.5		3.4		1.5		-	-	
	<b>Column</b>	Ext.	0.0	Ext.	0.0	Ext.	1.2	Ext.	2.5	Ext.	2.5
	<b>Beam</b>	Int.	5.4	Int.	3.7	Int.	1.7	Ext.	5.0	Ext.	5.0

		12-Story RC									
		NSP-1		NSP-2		NSP-3		(NTH, EQ-2)		(NTH, Mean)	
	<b>Global</b>		4.5		5.0		6.4		-	-	
Story-1	<b>Story</b>		7.3		9.6		12.9		-	-	
	<b>Column</b>	Ext.	8.3	Ext.	12.6	Ext.	16.5	Ext.	13.3	Ext.	8.2
	<b>Beam</b>	Ext.	8.4	Ext.	12.2	Ext.	17.2	Ext.	11.6	Ext.	5.8
Story-3	<b>Story</b>		5.8		6.1		6.8		-	-	
	<b>Column</b>		2.3	Ext.	1.9	Ext.	1.7	Ext.	1.6	Ext.	3.1
	<b>Beam</b>	Int.	7.7	Int.	7.5	Int.	10.0	Int.	7.5	Int.	6.2
Story-5	<b>Story</b>		5.4		4.6		3.6		-	-	
	<b>Column</b>	Ext.	1.4	Int.	2.0	Ext.	2.3	Ext.	2.5	Ext.	2.5
	<b>Beam</b>	Int.	7.0	Int.	5.3	Int.	3.4	Int.	6.7	Int.	5.8
Story-9	<b>Story</b>		2.4		1.1		-		-	-	
	<b>Column</b>	Ext.	0.0	Ext.	0.0	Int.	0.0	Int.	2.5	Int.	2.5
	<b>Beam</b>	Int.	2.6	Int.	1.1	Int.	0.0	Int.	2.5	Int.	3.8

Ext: Exterior; Int: Interior

In computing the ductility demands, the definition of yield rotation is important. For concrete structures, FEMA-356 suggests using an effective stiffness which defines the yield rotation at the yield moment. In this study, since a fiber section model is used for concrete members, the force-deformation response is non-linear even before yielding. Hence, the yield rotation was defined at the point where the moment magnitude reaches its yield value. For steel structures, FEMA-356 proposes an expression which assumes that the inflection point is at mid-length of the element. In the present paper, the following expression was used to estimate the yield rotation:

$$\theta_y = \frac{M_y^2 l}{3(M_y + M_2)EI} \quad (2)$$

where  $\theta_y$  is the yield rotation,  $M_2$  is the moment at one end of the member ( $M_2 < M_y$ ),  $l$  is the length of member,  $E$  is the elastic modulus,  $I$  is the moment of inertia, and  $M_y$  is the yield moment given by:

$$M_y = Zf_y \quad \text{for beams, and}$$

$$M_y = Zf_y \left( 1 - \frac{P}{A_g f_y} \right) \quad \text{for columns.}$$

In the above expressions,  $Z$  is the plastic modulus,  $P$  is the axial load,  $A_g$  is the gross area, and  $f_y$  is the yield strength of steel. In FEMA-356,  $M_2$  is assumed to be equal to  $M_y$ . This assumption is



reasonably true for beams in moment frame structures. For columns, the assumption of mid-point inflection leads to conservative estimates in pushover analyses. For time-history methods, the FEMA equation can sometimes lead to non-conservative values of the ductility demand. For example, the computed ductility using the FEMA expression in one case was 19.0 while using Equation (2) suggested above yields a ductility demand of 22.

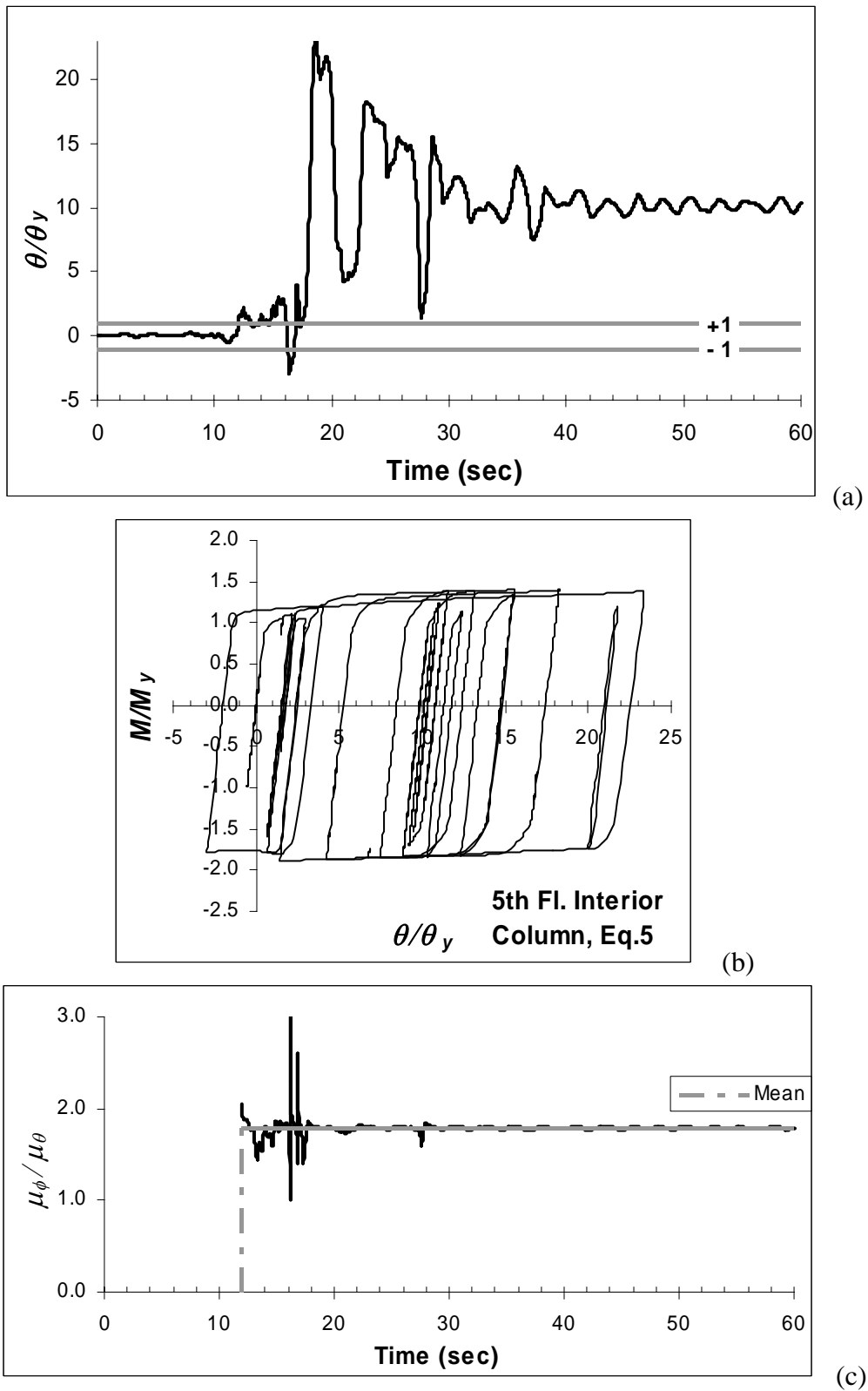


Fig. 13 Cyclic demand in typical column of 8-story steel building (time history response using Earthquake #5)

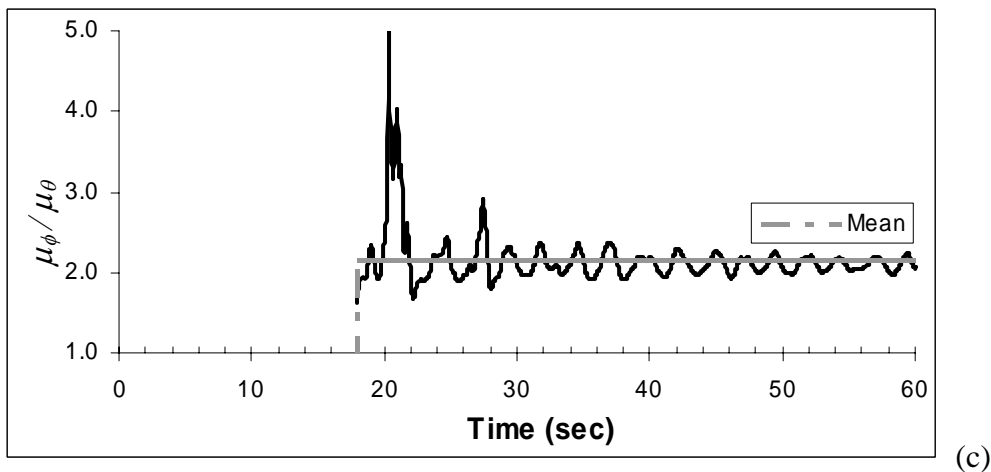
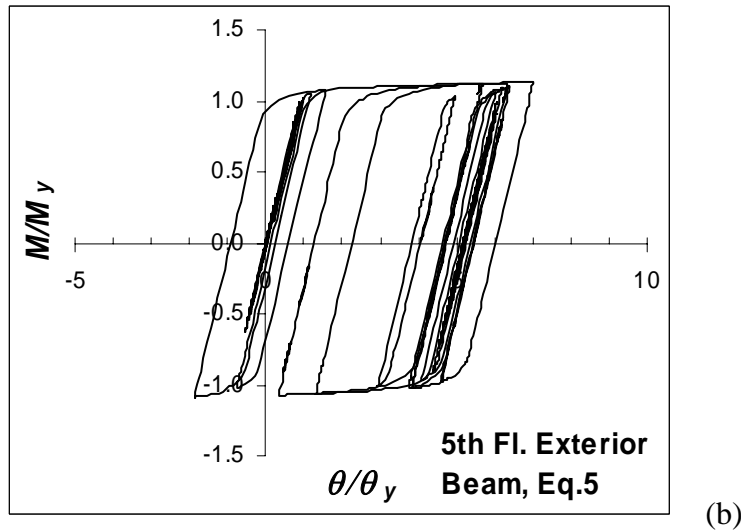
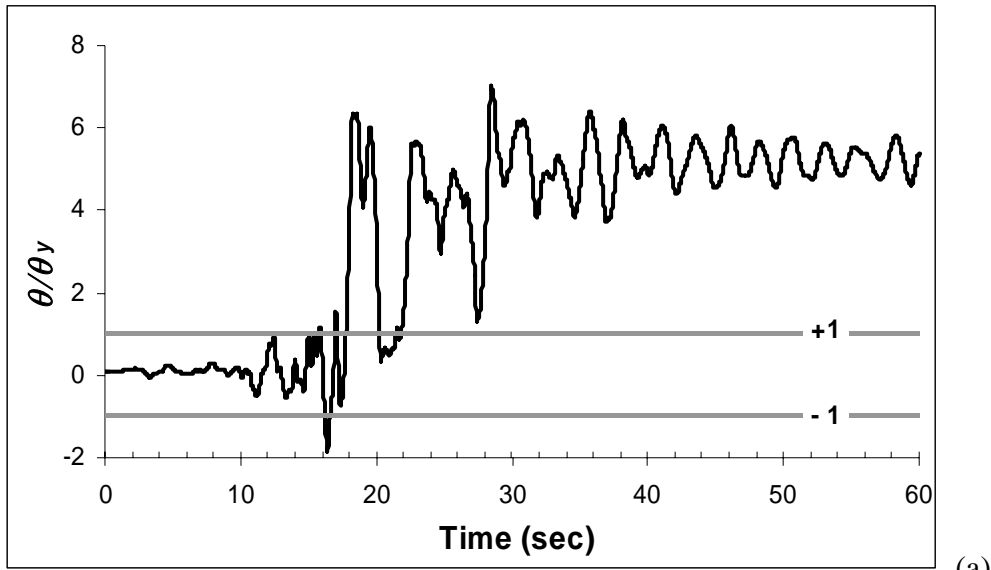


Fig. 14 Cyclic demand in typical beam of 8-story steel building (time history response using Earthquake #5)

**4. Further Implications of Using Component Demands to Evaluate Seismic Performance**

An issue that has not received much attention in performance-based seismic evaluation is the development of acceptance criteria. Currently, the performance of a building is governed by the performance of a single component in the system. Component performance is assessed on the basis of the peak ductility demand when non-linear procedures are used to estimate element deformations. The

consideration of peak values ignores the effect of cumulative damage resulting from cyclic deformations. The modeling of damage has been the subject of numerous research papers and a comprehensive review on the subject has been reported by Williams and Sexsmith (1995). Damage models have examined the process of component degradation and failure using measures of deformation, measures of dissipated energy or some combination of both. The damage model proposed by Park and Ang (1985), for example, uses a linear combination of deformation damage and damage resulting from cumulative effects. Studies utilizing the Park-Ang model have shown that most of the damage is a result of peak deformation rather than the effects of cumulative energy dissipation. Such conclusions reflect on the ability of the model to simulate cumulative effects rather than offer an insight into the cumulative damage process. It is necessary to examine studies on low-cycle fatigue behavior of components to appreciate the significance of this issue (Mander and Cheng, 1995; El-Bahy et al., 1999). Experimental tests carried out by El-Bahy et al. (1999) clearly show that both the energy and displacement capacity is a function of the number of cycles to which the component is subjected to at a given ductility level. Cyclic demand, therefore, is an important factor in performance-based engineering which seeks to delineate damage measures from elastic, undamaged state to post-yield response and failure. This aspect of demand is explored in this concluding section of the paper.

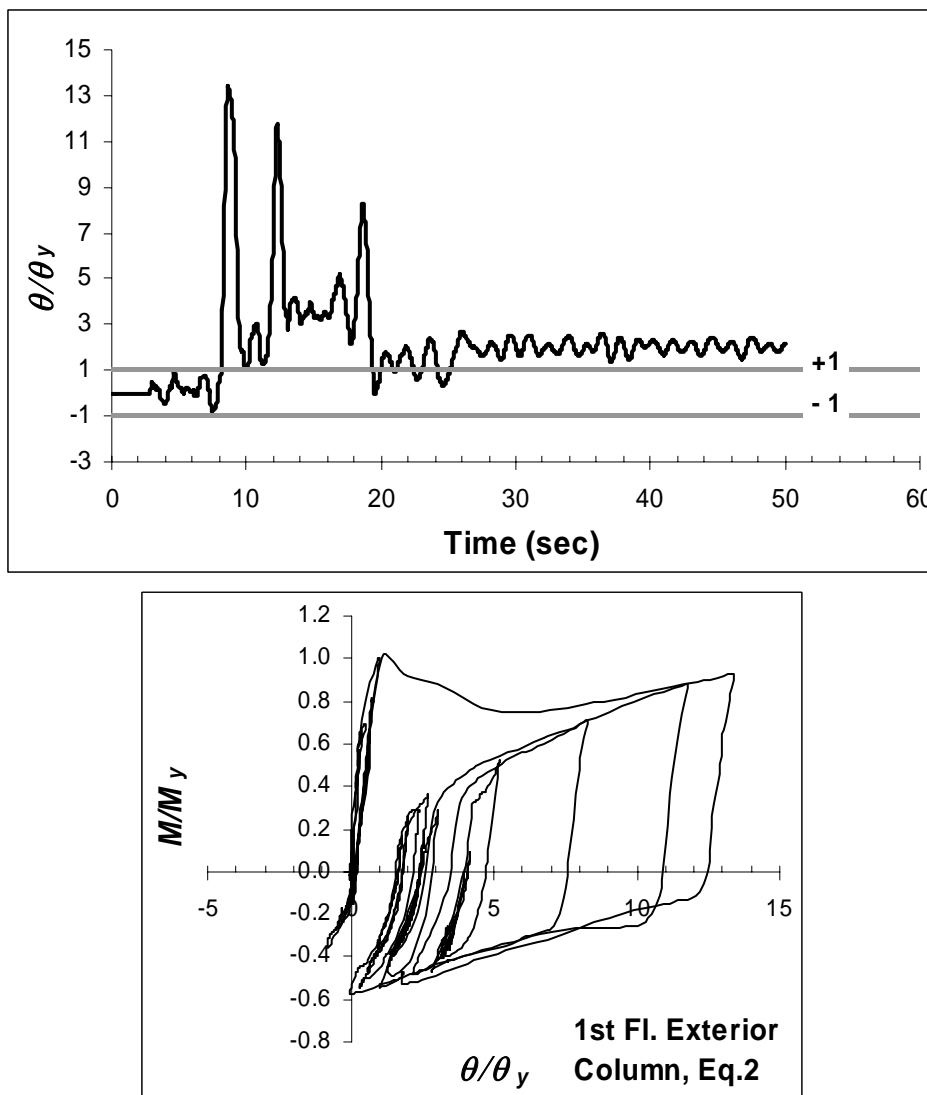


Fig. 15 Cyclic demand in typical column of 12-story RC frame

Figures 13–16 provide a glimpse of the implications of cyclic demand and the influence of low-cycle fatigue on performance assessment of structures. Figures 13 and 14 show a set of typical responses for a beam and column in the 8-story steel frame when subjected to an earthquake load. The ductility demand on the column using the peak rotation is 22.0. However, there are numerous additional cycles of deformation which exceed the yield rotation. Since the inelastic response results in a permanent drift, it is

more convenient to count the number of half cycles, wherein each half cycle is the peak-to-peak amplitude. If the peak-to-peak amplitude exceeds twice the yield rotation, that half cycle is considered to have exceeded the effective yield rotation and each such cycle is referred to as a “plastic cycle”. For the critical column shown in Figure 13, there were 17 half plastic cycles. Similarly, for the critical beam on the fifth floor of the 8-story steel frame, there were 16 half plastic cycles. The cumulative damage resulting from these cycles is much greater than implied by the peak ductility demand.

In addition to the cyclic demands, Figures 13 and 14 also include another useful piece of information: the relationship between curvature ductility and rotational ductility. Since curvature computations are localized, they exhibit large variations. The mean ratio of the curvature to rotational ductility is 1.85 for the column element and 2.2 for the beam element. This information is helpful in arriving at estimates of plastic hinge lengths when resorting to approximate methods to analyze structural frames.

Finally, cyclic demand data is presented for typical RC components in Figures 15 and 16. Axial force effects are evident in the response of the column element which experienced 9 half plastic cycles. The beam element, on the other hand, is subjected to 14 half plastic cycles. As pointed out earlier, the cumulative effects of these cycles cannot be ignored when assessing the performance of the component.

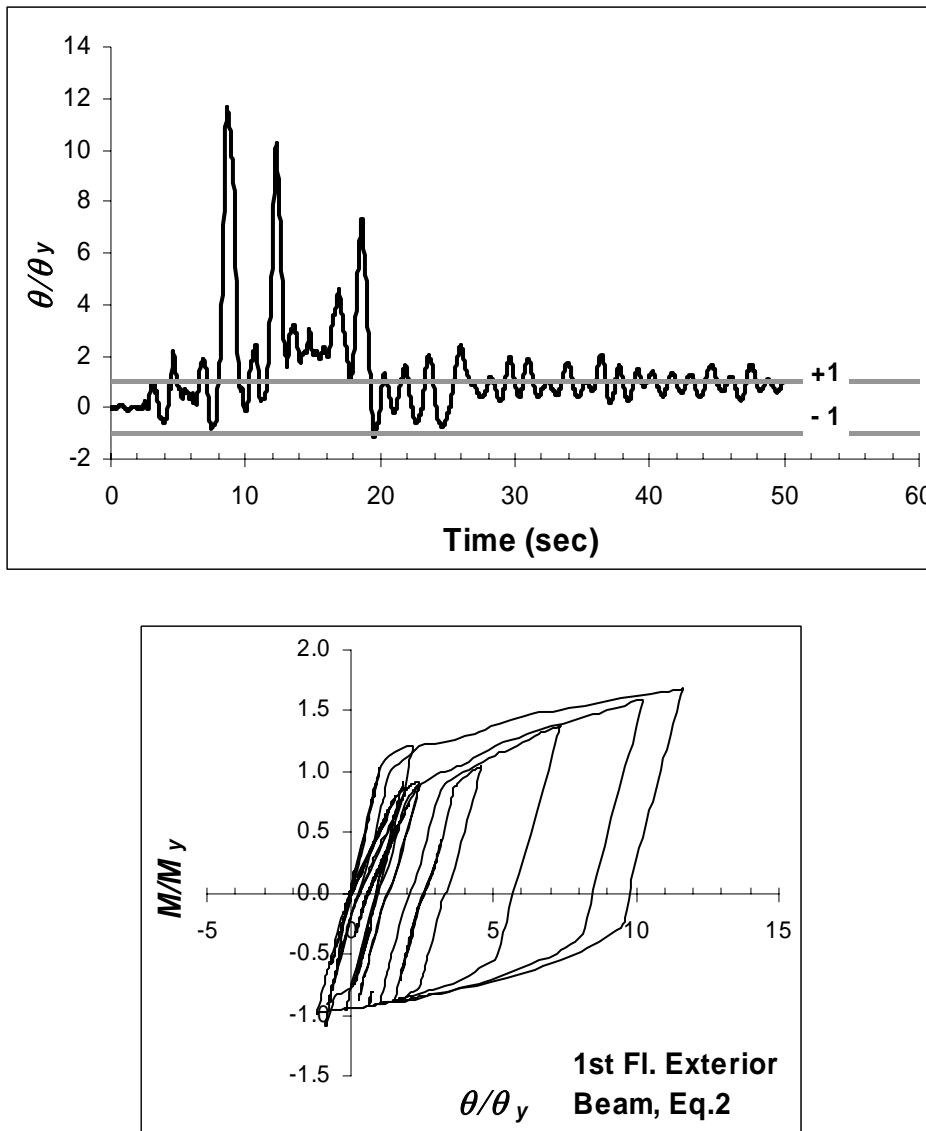


Fig. 16 Cyclic demand in a typical beam of 12-story RC frame

## FINDINGS AND CONCLUSIONS

Conventional seismic practice in the US is based on elastic procedures which rely on force reduction factors. Such an approach relies primarily on global demand estimates to evaluate the expected performance of a building. The emergence of FEMA-356 has now shifted the focus from global demand to local component demands. This paper attempts to raise questions on the validity of non-linear static approaches to estimate local demands and to explore correlations between component, story and global demands. The focus of this paper is not directly related to the assessment of design requirements rather it is an assessment of evaluation methods used to estimate seismic demands that play a major role in the design process. Pushover methods are undoubtedly an improvement over existing elastic force-based procedures and provide critical information on potential collapse mechanisms and the vulnerability for soft stories. For structures responding primarily in the first mode, non-linear static methods may be a reliable option to estimate inelastic demands.

Findings from this study indicate that there is no consistent correlation between demand estimates at the local, story and global level for the intensity level considered in the study. The evaluations presented here were based on seismic events with a 2% probability of being exceeded in 50 years. The demands at lower intensity levels could present a different picture considering the lower demands, hence similar evaluations for different intensity levels are needed to make generalized conclusions. Additionally, the inelastic models and the computational tools used to derive quantities such as plastic rotation also play an important role in establishing demand measures. It is generally assumed that the story demands are reasonably correlated to element demands at that story level. Some of the discrepancies between peak story demand and peak element demands suggest that additional scrutiny of the non-linear element models is needed before definitive conclusions can be reached on the reasons for this discrepancy.

Designing a building to achieve a certain ductility demand can result in much larger demands at the local level. Caution must be exercised when using non-linear static procedures since the lateral load pattern used to estimate demands can have a significant influence on the computed demands. When compared to non-linear time history estimates, pushover methods tend to underestimate demands at the upper levels signifying the relevance of high mode participation in mid to high rise structures. Non-linear response measures, using either static or dynamic analyses, are sensitive to modeling parameters such as the definition of effective stiffness, yield rotation, plastic hinge length, etc. and must be evaluated separately prior to utilizing the results of non-linear evaluations in performance assessment. Finally, demands based on peak values fail to take into consideration the cumulative effects of cyclic degradation. The quantification of cumulative effects is subject of ongoing studies by the authors.

This study was limited to standard invariant lateral load patterns recommended in FEMA-356. As indicated in the introductory section of the paper, methods exploring enhanced pushover methods which overcome many of the drawbacks of such procedures have been developed. The next step in this research effort is to evaluate local component demands using these new procedures. Previous studies, reported by Gupta and Kunnath (2000), and Chopra and Goel (2002), have been limited to investigation of inter-story demands. The present study has raised new questions related to the correlation between story demands and component demands and the computational tools used to estimate these quantities. Additional research is needed to address and clarify these issues.

## ACKNOWLEDGEMENTS

This study is supported by the National Science Foundation under Grant CMS-0296210, as part of the US-Japan Cooperative Program on Urban Earthquake Disaster Mitigation. Any opinions, findings, and conclusions or recommendations expressed in this material are those of the author(s) and do not necessarily reflect the views of the National Science Foundation.

## REFERENCES

1. ATC (1996). "Seismic Evaluation and Retrofit of Concrete Buildings", Report ATC-40 (also Report No. SSC 96-01, California Seismic Safety Commission), Applied Technology Council, Redwood City, CA, U.S.A.

2. Chopra, A.K. and Goel, R.K. (2002). "A Modal Pushover Analysis Procedure for Estimating Seismic Demands for Buildings", *Earthquake Engineering and Structural Dynamics*, Vol. 31, pp. 561-582.
3. Computers and Structures (2003). "SAP2000: Integrated Software for Structural Analysis and Design", Computers and Structures, Inc. (<http://csiberkeley.com>), Berkeley, CA, U.S.A.
4. Eberhard, M.O. and Sozen, M.A., (1993). "Behavior-Based Method to Determine Design Shear in Earthquake-Resistant Walls", *Journal of Structural Engineering*, ASCE, Vol. 119, No. 2, pp. 619-640.
5. El-Bahy, A., Kunnath, S.K., Stone, W.C. and Taylor, A.W. (1999). "Cumulative Seismic Damage of Circular Bridge Columns", *ACI Structural Journal*, Vol. 96, No. 4, pp. 633-641.
6. Fajfar, P. and Fischinger, M. (1988). "N-2 – A Method for Nonlinear Seismic Analysis of Regular Structures", *Proceedings of 9th US National Conference on Earthquake Engineering*, Tokyo-Kyoto, Japan.
7. FEMA (2000a). "Recommended Seismic Design Criteria for New Steel Moment-Frame Buildings", Report FEMA-350, Federal Emergency Management Agency, Washington DC, U.S.A.
8. FEMA (2000b). "Prestandard and Commentary for the Seismic Rehabilitation of Buildings", Report FEMA-356, Federal Emergency Management Agency, Washington, DC, U.S.A.
9. Freeman, S.A. (1978). "Prediction of Response of Concrete Buildings to Severe Earthquake Motion" in "Proceedings of Douglas McHenry International Symposium on Concrete and Concrete Structures", Publication No. SP-55, American Concrete Institute, Detroit, pp. 589-605.
10. Gupta, B. and Kunnath, S.K. (2000). "Adaptive Spectra-Based Pushover Procedure for Seismic Evaluation of Structures", *Earthquake Spectra*, Vol. 16, No. 2, pp. 367-392.
11. Iwan, W.D. (1999). "Implications of Near-Fault Ground Motion for Structural Design", *Proceedings of US-Japan Workshop on Performance-Based Earthquake Engineering Methodology for RC Building Structures*, Maui, Hawaii, U.S.A. (available from PEER, UC Berkeley, U.S.A.).
12. Krawinkler, H. and Seneviratna, G.D.P.K. (1998). "Pros and Cons of a Pushover Analysis for Seismic Performance Evaluation", *Engineering Structures*, Vol. 20, No. 4-6, pp. 452-464.
13. Kunnath, S.K. and Gupta, S.K. (2000). "Validity of Deformation Demand Estimates Using Nonlinear Static Procedures", *Proceedings of US-Japan Workshop on Performance-Based Earthquake Engineering Methodology for RC Building Structures*, Sapporo, Japan.
14. Kunnath, S.K. and John Jr., A. (2000). "Validity of Static Procedures in Performance-Based Seismic Design", *Proceedings of ASCE Structures Congress*, Philadelphia, U.S.A.
15. Mander, J.B. and Cheng, C.-T. (1995). "Renewable Hinge Detailing for Bridge Columns", *Proceedings of Pacific Conference on Earthquake Engineering*, Melbourne, Australia.
16. Mwafy, A.M. and Elnashai, A.S. (2001). "Static Pushover versus Dynamic Collapse Analysis of RC Buildings", *Engineering Structures*, Vol. 23, No. 5, pp. 407-424.
17. OpenSees (2003). "Open System for Earthquake Engineering Simulation", <http://opensees.berkeley.edu>.
18. Park, Y.J. and Ang, A.H.-S. (1985). "Mechanistic Seismic Damage Model for Reinforced Concrete", *Journal of Structural Engineering*, ASCE, Vol. 111, No. ST4, pp. 722-739.
19. Sasaki, K.K., Freeman, S.A. and Paret, T.F. (1998). "Multimode Pushover Procedure (mmP) – A Method to Identify the Effects of Higher Modes in a Pushover Analysis", *Proceedings of 6th US National Conference on Earthquake Engineering*, Seattle, U.S.A.
20. Satyarno, I., Carr, A.J. and Restrepo, J. (1998). "Refined Pushover Analysis for the Assessment of Older Reinforced Concrete Buildings", *Proceedings of New Zealand National Society for Earthquake Engineering Technical Conference*, Wairakei, New Zealand, pp. 75-82.
21. SEAOC (2000). "Seismic Design Manual, Volume III – Building Design Examples: Steel Concrete and Cladding", Structural Engineers Association of California, Sacramento, CA, U.S.A.
22. Tso, W.K. and Moghadam, A.S. (1998). "Pushover Procedure for Seismic Analysis of Buildings", *Progress in Structural Engineering and Materials*, Vol. 1, No. 3, pp. 337-344.
23. Wight, J.K., Burak, B., Canbolat, B.A. and Liang, X. (1999). "Modeling and Software Issues in Pushover Analysis of RC Structures" in "Proceedings of US-Japan Workshop on Performance-Based

Earthquake Engineering Methodology for Reinforced Concrete Building Structures”, Report PEER-1999/10, Pacific Earthquake Engineering Research Center, Berkeley, CA, U.S.A.

24. Williams, M.S. and Sexsmith, R.G. (1995). “Seismic Damage Indices for Concrete Structures: A State-of-the-Art Review”, *Earthquake Spectra*, Vol. 11, No. 2, pp. 319-350.